15 Years: Top Quality, No Price Increases

Celebrating 15 Years

2002 2003 2004 2005 2006 2007 2008 2009 2010 2011 2012 2013 2014 2015 2016 2017

BioLegend®

The Journal of Immunology

Nitrotyrosine Proteome Survey in Asthma Identifies Oxidative Mechanism of Catalase Inactivation

Sudakshina Ghosh, Allison J. Janocha, Mark A. Aronica, Shadi Swaidani, Suzy A. A. Comhair, Weiling Xu, Lemin Zheng, Suma Kaveti, Michael Kinter, Stanley L. Hazen and Serpil C. Erzurum

---

References	This article **cites 74 articles**, 27 of which you can access for free at: http://www.jimmunol.org/content/176/9/5587.full#ref-list-1
Subscription	Information about subscribing to *The Journal of Immunology* is online at: http://jimmunol.org/subscription
Permissions	Submit copyright permission requests at: http://www.aai.org/About/Publications/JI/copyright.html
Email Alerts	Receive free email-alerts when new articles cite this article. Sign up at: http://jimmunol.org/alerts

Nitrotyrosine Proteome Survey in Asthma Identifies Oxidative Mechanism of Catalase Inactivation[1]

**Sudakshina Ghosh,*† Allison J. Janocha,*† Mark A. Aronica,*† Shadi Swaidani,*†
Suzy A. A. Comhair,*† Weiling Xu,*† Lemin Zheng,‡ Suma Kaveti,‡ Michael Kinter,‡
Stanley L. Hazen,‡§ and Serpil C. Erzurum[2]*†**

Reactive oxygen species and reactive nitrogen species produced by epithelial and inflammatory cells are key mediators of the chronic airway inflammation of asthma. Detection of 3-nitrotyrosine in the asthmatic lung confirms the presence of increased reactive oxygen and nitrogen species, but the lack of identification of modified proteins has hindered an understanding of the potential mechanistic contributions of nitration/oxidation to airway inflammation. In this study, we applied a proteomic approach, using nitrotyrosine as a marker, to evaluate the oxidation of proteins in the allergen-induced murine model of asthma. Over 30 different proteins were targets of nitration following allergen challenge, including the antioxidant enzyme catalase. Oxidative modification and loss of catalase enzyme function were seen in this model. Subsequent investigation of human bronchoalveolar lavage fluid revealed that catalase activity was reduced in asthma by up to 50% relative to healthy controls. Analysis of catalase isolated from asthmatic airway epithelial cells revealed increased amounts of several protein oxidation markers, including chloro- and nitrotyrosine, linking oxidative modification to the reduced activity in vivo. Parallel in vitro studies using reactive chlorinating species revealed that catalase inactivation is accompanied by the oxidation of a specific cysteine (Cys^{377}). Taken together, these studies provide evidence of multiple ongoing and profound oxidative reactions in asthmatic airways, with one early downstream consequence being catalase inactivation. Loss of catalase activity likely amplifies oxidative stress, contributing to the chronic inflammatory state of the asthmatic airway. *The Journal of Immunology,* **2006, 176: 5587–5597.**

Asthma is a chronic disease of airway inflammation, characterized by reversible airflow obstruction and bronchial hyperresponsiveness (1). Reactive oxygen species (ROS)[3] and reactive nitrogen species (RNS) produced by inflammatory and epithelial cells are believed to be key mediators of asthmatic airway inflammation (2–4). High levels of RNS are well documented in asthma (5, 6), e.g., NO is higher in exhaled breath of asthmatics than healthy controls (7–10). NO synthases (NOS; neuronal, inducible, and endothelial) produce NO, and all isoforms are present in the lung (7, 8, 11, 12), but high levels of NO in asthma are linked to increased inducible NOS (iNOS) expression and activity in airway epithelial cells (8). Previous studies also confirm increased ROS production in the airways and circulation of asthmatic subjects (5, 13, 14). In particular, eosinophils and

monocytes from asthmatic patients produce more ROS than cells from healthy controls (14).

During asthma exacerbation, infiltration of the lung with eosinophils and neutrophils results in elevated levels of various peroxidases, such as eosinophil peroxidase and myeloperoxidase (MPO) (17). These peroxidases use chlorine and bromine, present in tissues, to form the hypohalous acids HOCl and HOBr (16, 18, 19). These hypohalous acids are potent oxidants and contribute to the cidal activities of phagocytic cells (14, 15), in the process chlorinating and brominating protein tyrosines to form 3-chlorotyrosine (Cl-Y) and 3-bromotyrosine (16), specific markers of MPO and eosinophil peroxidase activity, respectively. MPO also uses the oxidation of nitrite (an oxidation product of NO) to generate nitrogen dioxide radical (5, 17, 18) to nitrate protein tyrosine and form 3-nitrotyrosine (5, 19–21). Thus, enhanced formation of NO-derived oxidants occurs within the airway through several mechanisms. The detection of 3-nitrotyrosine and 3-Cl-Y in the lung during asthma attacks provides definitive evidence for the presence of high levels of RNS and ROS in the asthmatic airway (5, 17, 22, 23).

We hypothesized that identification of specific oxidized proteins would provide mechanistic information regarding oxidative stress and insight into downstream functional consequences. For example, the identification of nitrated proteins, and consequences of ROS and RNS on protein function, has provided a greater depth of knowledge into the molecular pathophysiologic mechanisms in neurodegenerative and cardiovascular diseases (24–29). In this study, nitrotyrosine was used as a general marker for protein exposure to oxidant stress. Specific proteins were identified as preferential targets of modification in the asthmatic condition, including the antioxidant proteins catalase and manganese superoxide dismutase (MnSOD). Parallel functional studies in a murine model of asthma revealed a significant loss of lung catalase activity, and

*Department of Pathobiology, †Department of Pulmonary, Allergy and Critical Care Medicine, ‡Department of Cell Biology, and §Center for Cardiovascular Diagnostics and Prevention, Department of Cardiovascular Medicine, Cleveland Clinic Foundation, Cleveland, OH 44195

[2] Address correspondence and reprint requests to Dr. Serpil C. Erzurum, Chair, Department of Pathobiology, Cleveland Clinic Foundation, 9500 Euclid Avenue/NC22, Cleveland, OH 44195. E-mail address: erzurus@ccf.org

[3] Abbreviations used in this paper: ROS, reactive oxygen species; RNS, reactive nitrogen species; NOS, NO synthase; iNOS, inducible NOS; MPO, myeloperoxidase; Cl-Y, chlorotyrosine; MnSOD, manganese superoxide dismutase; LC, liquid chromatography; MS, mass spectrometry; BALF, bronchoalveolar lavage fluid; ELF, epithelial lining fluid; NO_X, nitrite and nitrate; eNOS, endothelial NOS; Cu-ZnSOD, copper-zinc superoxide dismutase; CID, collision-induced dissociation.

the loss of catalase activity was verified in the airway of human asthmatic subjects. Finally, liquid chromatography (LC)-tandem mass spectrometry (MS) and MALDI-TOF analysis of an in vitro reaction of catalase with reactive chlorinating species revealed a unique modification, the oxidation of Cys[377], which correlated with the loss of enzyme activity. Taken together, these studies provide evidence of ongoing profound oxidative processes in asthmatic airways, with the downstream consequence of catalase inactivation, which likely amplifies inflammation in the asthmatic airway.

Materials and Methods

Allergen sensitization, methacholine challenge, and lung analyses

Induction of murine asthma and bronchoalveolar lavage analysis was performed as described previously (30). BALB/c mice (6- to 8-wk-old) from The Jackson Laboratory were immunized (i.p.) with OVA (Sigma-Aldrich) in aluminum hydroxide (10 μg of OVA/20 μg of aluminum hydroxide). Two weeks later, mice were challenged with OVA aerosol for 40 min each day. Samples were collected 24 h following the final aerosol inhalation at day 0, 2, 4, 6, and 8. To measure lung resistance in response to methacholine challenge, mice were anesthetized and placed on a rodent ventilator inside a body plethysmography chamber. After a stable baseline pressure was established, mice were given three serially increasing doses of methacholine (45–411 μg/kg in a volume of 40–55 μl/dose). Methacholine doses were i.v. administered by intrajugular catheter 5 min apart and only after transpulmonary pressure and volume returned to baseline. Resistance and compliance were determined using Buxco electronics and Biosystems XA software. Methacholine dose-response curves were obtained by calculating the mean $\pm$ SE for individual animals at each methacholine dose (data not shown). The mice were sacrificed, lungs were lavaged with normal saline, and cytological examination was performed. Differential counts were based on counts of 100 cells using standard morphologic criteria to classify the cells. A single observer who was blinded to the study group performed counts. Tissues were collected and frozen rapidly in liquid nitrogen until needed.

Human bronchial epithelial cells and bronchoalveolar lavage fluid (BALF)

Healthy controls ($n = 19$) and asthmatic individuals ($n = 11$) underwent bronchoscopy to obtain BALF and bronchial epithelial cells as described previously (31, 32). Clinical characteristics of asthmatics were similar to controls (age (years), asthmatic 36 ± 2, control 37 ± 2; $p > 0.05$; percentage of predicted forced expiratory volume in 1 s, asthmatic 87 ± 4, control 98 ± 5; $p > 0.05$). None of the participants in the study were current users of tobacco products. All controls were nonsmokers and were recruited such that they had never smoked, or had less than a total 5-pack year history of smoking with no smoke exposure in over 10 years. Urea was determined in BALF and serum using the Blood Urea Nitrogen (BUN ENDPOINT; Sigma-Aldrich) reaction (32) and relative level of epithelial lining fluid (ELF) estimated by simple dilution principles relating to the urea concentration in serum and BALF (33). The study was approved by the institutional review board, and written informed consent was obtained from all individuals enrolled in the study.

Measurement of total NO reaction products

Nitrite and nitrate (NO_X) concentrations were determined in replicate samples using the ISO-NOP Nitric Oxide Sensor (World Precision Instruments) as described previously (34).

Cell culture

RAW 264.7 cells were grown to 70% confluency in RPMI1640 medium with 5% FCS (35). After 18-h treatment with LPS (1 μg/ml), the cells were washed in PBS and harvested in SDS-PAGE lysis buffer.

Enzyme activity

Quantitation of catalase activity was based on reaction with H_2O_2 (36). The activity was expressed as U/mg total protein in murine lung tissues or as mU/ml ELF in human BALF.

Immunohistochemistry

Formalin-fixed, paraffin-embedded (5 μm) sections were treated with polyclonal anti-nitrotyrosine Ab (Upstate Biotechnology; 1/400 dilution). Im-

munohistochemical staining was performed by an avidin-biotin alkaline phosphatase system (Vector Laboratories) (37). For negative control, the sections were incubated with secondary Ab alone.

In vitro modification of catalase

Isolated human erythrocyte catalase (Oxis Research) was exposed to reactive chlorinating species in vitro by treatment with HOCl (0–100 μM) at 37°C (29) and nitrating species by 12 mM tetranitromethane (Sigma-Aldrich) at room temperature for 30 min. Catalase, modified by nitration, was used as a positive control in immunoprecipitation studies. Unmodified catalase served as negative control.

Aminotriazole treatment and MPO modification of catalase

Isolated human erythrocyte catalase was inactivated by aminotriazole (Sigma-Aldrich) (38), and excess aminotriazole was removed by dialysis before MPO-mediated reaction. MPO-mediated modification reactions were conducted with 500 μg/ml aminotriazole-inactivated catalase in 60 mM phosphate buffer (pH 7.0), containing 100 μM diethylenetriamine pentaacetic acid, 57 nM purified MPO, prepared as described previously (28). The reactions were initiated by adding H_2O_2 at varying concentrations (0–150 μM). These reaction conditions include concentrations of MPO, chloride, and H_2O_2 at ranges from physiologic to pathologic (29).

Immunoprecipitation

Ig was first removed from human airway epithelial cell lysate with protein G-Sepharose (Amersham Pharmacia). Supernatants were incubated with polyclonal anti-catalase Ab (Oxisresearch), then protein G-Sepharose was added and incubated at 4°C for 2 h. The proteins captured by the beads were extracted in denaturing-nonreducing buffer, analyzed for anti-nitrotyrosine immunoreactivity, and reblotted with anti-catalase after stripping.

Similarly, mouse lung lysates were immunoprecipitated with anti-iNOS Ab. The captured proteins were extracted in denaturing-reducing buffer and analyzed for anti-iNOS immunoreactivity.

Two-dimensional gel electrophoresis

Two-dimensional gel electrophoresis was performed with the isoelectric-focusing system (Bio-Rad), using 11-cm linear (pH 3–10) immobilized pH gradient strips. Strips were rehydrated with sample (500 μg) at 50 V for 14 h, and then isoelectric-focusing system was performed according to manufacturer's instruction. The second dimension was performed according to Laemmli (39). Finally, gels were partially transferred to the polyvinylidene difluoride membrane (40) to detect anti-nitrotyrosine immunoreactivity. Gels were stained with colloidal Coomassie blue (Gel Code Blue Stain; Pierce).

Western blot analysis

Tissues were homogenized in lysis buffer, separated on 10% SDS-polyacrylamide gels, and transferred to polyvinylidene difluoride membrane. After blocking in 5% milk at room temperature, membranes were incubated overnight with primary Ab at 4°C. Then blots were probed with a peroxidase-conjugated secondary Ab, and signal was detected by enhanced chemiluminescent system (ECL; Amersham Bioscience). The primary Abs were polyclonal anti-catalase (Oxisresearch), polyclonal anti-iNOS Ab (Upstate Biotechnology), polyclonal anti- endothelial NOS (eNOS) Ab (Affinity Bioreagents), polyclonal anti-Cu-ZnSOD (copper-zinc superoxide dismutase), polyclonal anti-MnSOD, polyclonal anti-arginase I, and polyclonal anti-β-actin Ab (Santa Cruz Biotechnology). For anti-nitrotyrosine detection, the blots were blocked in 2% BSA, followed by overnight incubation with anti-nitrotyrosine mAb (Upstate Biotechnology) at 4°C, and then with peroxidase-linked anti-mouse secondary Ab.

Protein identification

Anti-nitrotyrosine-positive spots were matched with the Coomassie-stained two-dimensional gel and identified according to our standard MS procedures (41). Briefly, the selected protein spots were processed and rehydrated in ice-cold sequencing-grade trypsin (Promega). The peptides produced were extracted and analyzed using a full data-dependent acquisition routine in which a full-scan MS to determine peptide molecular masses was acquired in one scan, and product-ion (tandem mass) spectra to determine amino acid sequence were acquired in the four subsequent scans before repeating the cycle. The resulting MS/MS spectra were automatically batch-analyzed using the search program Mascot (⟨http://www.matrixscience.com⟩). To identify sites of modifications, the Sequest program was used to compare CID spectra of catalase to the database (National Center for Biotechnology
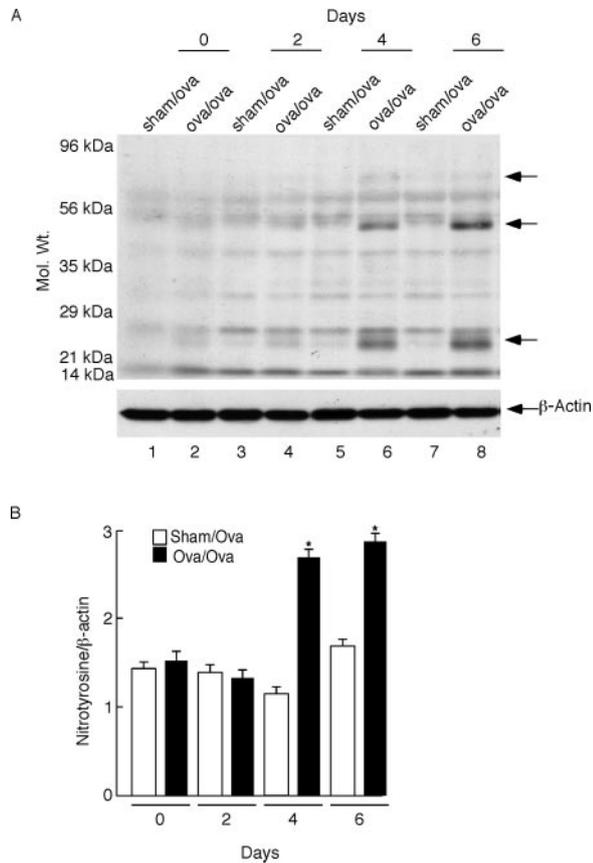
FIGURE 1. Increased nitrotyrosine in OVA-sensitized and challenged mouse lung. *A*, Western blot analysis of nitrotyrosine in tissue lysate of asthmatic mouse lung at days 0, 2, 4, and 6 (*lanes 1, 4, 6,* and *8*) and corresponding controls at respective days (*lanes 1, 3, 5,* and *7*) revealed more nitration in asthmatic lungs compared with controls. *Lower panel* is β-actin Western analyses for loading control. All data are representative of at least three experiments. *B*, Densitometric analysis of the Western blots shows that total nitrotyrosine band intensity compared with β-actin is significantly increased in asthmatic lung compared with control. ∗, Indicates *p* < 0.05.

FIGURE 2. iNOS, eNOS, and arginase expression in asthmatic mouse lung. *A*, At 0, 2, 4, and 6 days of study, control (*lanes 1, 3, 5,* and *7*) and asthmatic mouse lung lysates (*lanes 2, 4, 6,* and *8*) were evaluated by Western analyses for arginase I and eNOS, and immunoprecipitation for iNOS before running on SDS-PAGE. Lysates from RAW 264.7 cells stimulated with LPS (*first panel, last lane*) and mouse liver (*second panel, last lane*), respectively, served as positive control for iNOS and arginase I. All data are representative of at least three experiments. *B*, Densitometric analysis of the Western blot data shows iNOS and arginase I are significantly increased, whereas eNOS is not significantly altered. ∗, Indicates *p* < 0.05.

Information, accession no. AAA66054) using the appropriate mass change for the different amino acid oxidation products (42).

Quantitation of purified catalase for protein-bound oxidation and nitration

Catalase was immunoprecipitated, and protein L gel slurry (Pierce) was added to deplete Ig. Purified catalase was precipitated by acetone and dried in nitrogen. Protein-bound nitrotyrosine, Cl-Y, bromotyrosine, dityrosine, orthotyrosine, and metatyrosine were quantified by stable isotope dilution LC-tandem MS using methods as described previously (28). Isolated catalase, modified in vitro (by HOCl or MPO-mediated system), was also quantitatively analyzed for total and specific modifications.
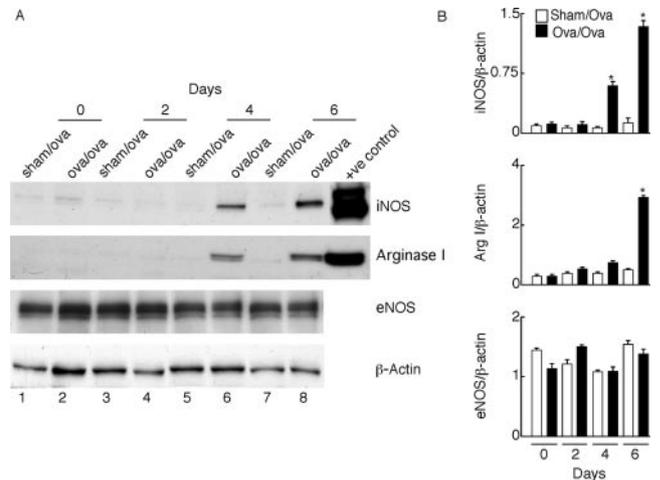
Statistical analysis

All data are expressed as the mean ± SEM. The comparisons between the groups were performed using ANOVA or Student's *t* test.

Results

Differential cell count in the BALF of OVA-sensitized and challenged mice

BALB/c mice were sensitized using OVA in aluminum hydroxide, then rechallenged by repeated inhalation of OVA. Measurement of lung airway resistance at different doses of methacholine challenge showed that airway resistance increased starting at day 4 of allergen challenge (lung resistance in cm/H_2O/ml/s: baseline, 1.51 ±

0.05; 411 μg methacholine/kg body weight of mice, 5.58 ± 0.23; *p* < 0.05) (43). Mice were sacrificed 24 h following the final aerosol inhalation at each of days 0, 2, 4, 6, or 8. Consistent with previous studies of this model (44–46), OVA-sensitized and challenged mice developed a marked inflammatory response to OVA, with evidence of infiltrates composed predominantly of eosinophils and a lesser component of mononuclear cells (total number of cells and eosinophils at day 0: total 12 ± 1, eosinophils 0; day 2: total 25 ± 5, eosinophils 11 ± 2; day 4: total 101 ± 35, eosinophils 68 ± 28; day 6: total 155 ± 40, eosinophils 124 ± 31). Control mice did not show a significant amount of cell infiltration at any day studied. Mice sacrificed at day 6 showed maximum eosinophil infiltration (124 ± 31; ANOVA, *p* < 0.01) with a sparse admixture of neutrophils and lymphocytes.

Increased reactive nitrogen species in OVA-sensitized and challenged mice compared with control
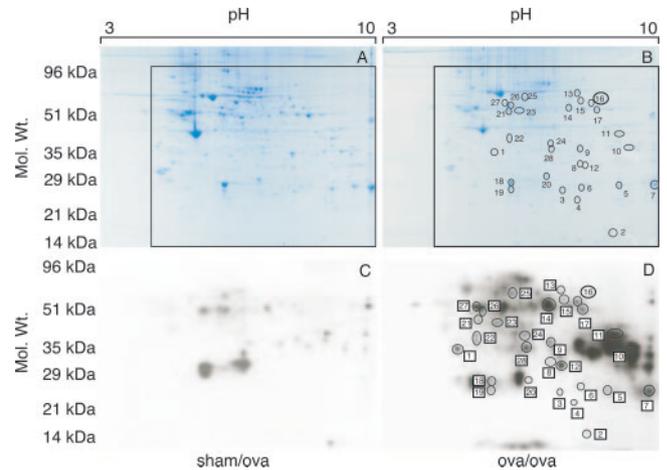
We examined the extent and range of protein nitration by Western blot analysis using specific monoclonal anti-nitrotyrosine Ab at day 0, 2, 4, and 6 of allergen challenge (*n* = 3 mice at each time). Multiple bands representing nitrated protein were detected at day 4 and increased at day 6 following OVA challenge in sensitized mice compared with control (Fig. 1*A*). However, nitrotyrosine-positive bands were not detected at day 0 and 2 of allergen challenge. The increase in nitrotyrosine-positive bands was apparent in the molecular mass range of 21–96 kDa. In contrast to nitrotyrosine, total NO_X in OVA-sensitized and challenged mice lung lavage at days 4 and 6 were similar to control mice lung lavage (NO_X μM at day 4: OVA/OVA 2.0 ± 0.2, sham/OVA 2.5 ± 0.2; *p* = 0.7; NO_X at day 6: OVA/OVA 2.5 ± 0.4, sham/OVA 2.7 ± 0.3; *p* = 0.16). The lack of increase of NO_X suggested that NO synthesis might not increase over time of allergen-induced airway inflammation. Alternatively, NO synthesis may have increased, but consumption of NO by oxidants/peroxidases and incorporation into 3-nitrotyrosine may have been greater than NO synthetic rate.
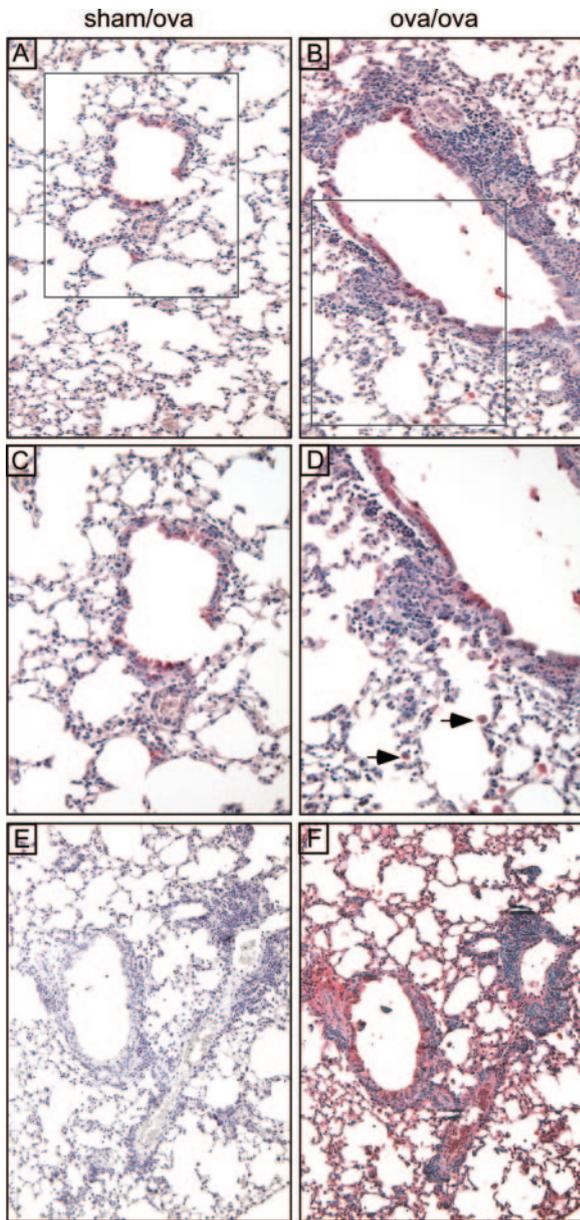
FIGURE 3. Immunohistochemical staining of asthmatic mouse lung. Epithelial cells surrounding the asthmatic airway (*B*) show positive immunoreactivity to nitrotyrosine (red), whereas corresponding control (*A*) is barely positive (×10). Presence of inflammatory cells are shown by arrow in *D*, magnified view (×20) of *B*, which is absent in control (*C*; ×20). *E* and *F* are the negative and positive controls for staining, respectively (×10; hematoxylin counterstaining). All data are representative of at least three experiments.

FIGURE 4. Two-dimensional patterns of anti-nitrotyrosine-immunopositive protein in asthmatic mouse lung compared with control at day 6. Lung tissue samples from control and OVA/OVA mice were subjected to proteomic analysis. Coomassie blue-stained polyacrylamide gels of control (*A*) and OVA/OVA mouse lung tissue (*B*) are shown with the corresponding Western blots (*bottom panel*, *C* and *D*, respectively). Although the control blot (*C*) shows some degree of nitration, the blot (*D*) representing the profile of OVA/OVA mouse lung shows more intense nitration. The protein spots, corresponding to the immunoreactive proteins observed in Western blot (*D*) on Coomassie-stained gel (*B*), were identified by tandem MS. All data are representative of at least three experiments.

viously identified in lung lysate of OVA-sensitized and challenged mice (47). Arginase can compete with NOS for substrate arginine use, and hence affect NO and RNS synthesis (48, 49). In this study, Western analysis with anti-arginase I Ab revealed that there was significant increase of arginase I in OVA-sensitized and challenged mice at days 4 and 6 of allergen challenge compared with the control (Fig. 2*A*).

Immunohistochemistry for anti-nitrotyrosine

Because there was maximum eosinophil infiltration and significant protein nitration at day 6 of allergen challenge, this time point was chosen for further studies. Because of the heterogeneous nature of lung tissue and inflammatory changes occurring during sensitization and challenge, immunohistochemical staining was performed to localize nitrotyrosine immunoreactivity. Positive immunoreactivity for nitrotyrosine, a collective marker for ROS and RNS, was observed in the airway epithelial cells of OVA-sensitized and challenged mice at day 6 of allergen challenge (*n* = 3) (Fig. 3). As previously shown (50, 51), these results support the presence of ROS and RNS generation mainly within the airway epithelium and inflammatory cells of the sensitized and challenged lung.

Proteomic analysis of anti-nitrotyrosine immunopositive proteins in OVA-sensitized and challenged mouse lung

Protein from control and asthmatic murine lung homogenate was separated by two-dimensional gel electrophoresis. Comparison of Coomassie-stained two-dimensional gel of control and OVA-sensitized and challenged lung did not show any significant changes in the protein profile; however, Western blot with anti-nitrotyrosine Ab revealed that there was intense protein nitration in OVA-sensitized and challenged lung compared with control (Fig. 4). Control lung had immunopositive spots (19 ± 5), but the number of spots (49 ± 9) and the intensity of specific spots was higher in the OVA-sensitized and challenged lung. For OVA-sensitized and challenged lungs, corresponding immunopositive proteins were

iNOS and eNOS expression in OVA-sensitized and challenged mice compared with control

To investigate ·NO synthesis, iNOS protein expression was evaluated. Whole lung lysate (400–600 μg of total protein) of control and OVA-sensitized and challenged mice (*n* = 3 at each time point) were immunoprecipitated with anti-iNOS Ab. The immunocomplex was resolved in 10% gel, and the immunoblot was probed with anti-iNOS Ab. A protein (130 kDa) in OVA-sensitized and challenged mice lung lysate was detected at days 4 and 6, which was similar in size to iNOS in positive control lysate from RAW 264.7 cells stimulated with LPS (Fig. 2*A*). Western analysis with anti-eNOS Ab revealed that the expression of this protein was similar throughout all days studied. Arginase expression was pre-

excised from the parent acrylamide gel, digested in-gel with trypsin, and tryptic peptides were analyzed with mass spectroscopy. Database searching with the peptide masses identified the majority of immunopositive spots (Table I).

Expression and activity of antioxidant proteins in OVA-sensitized and challenged mouse lung

Many of the nitrated proteins identified were related to antioxidant defense. To determine whether the levels of antioxidant proteins were increased in OVA-sensitized and challenged mice compared with control, catalase, Cu-ZnSOD, and MnSOD protein expression were evaluated by Western analysis at day 0, 2, 4, and 6 of allergen

challenge ($n = 3$ at each time). There was no significant change in expression of any of the proteins at any time (Fig. 5A). Despite comparable levels of catalase mass, activity of catalase in tissue homogenate was decreased significantly in OVA-sensitized and challenged mice compared with control at days 4 and 6 of allergen challenge (Fig. 5B).

Catalase in human asthma

Catalase activity was decreased on average by 50% in human asthmatic BALF as compared with controls (catalase mU/ml ELF: control, 149 ± 27 ($n = 6$); asthma, 70 ± 20 ($n = 7$); $p < 0.05$) (Fig. 6A). However, catalase expression in cell lysates of airway

Table I. *Identification of nitrated proteins in OVA-sensitized and challenged mice[a]*

No.[b]	Proteins	pL	Molecular Mass (kDa)	Accession No.	Coverage	No. of Peptides Matched	Function
1	Annexin III	5.6	36	CAA04887	62%	54	Associated with cytoplasmic granules in neutrophils and monocytes and translocates to the plasma membrane in activated cells
2	HBβ-chain	8.5	14	XP_489729	38%	9	Subunit of hemoglobin
	Profilin	8.5	14	CAB87382	79%	39	Regulates actin polymerization in response to extracellular signals
3	GTP-binding protein	7	24	BAA01555	23%	20	Involved in signal transduction
4	MnSOD	8.6	24	CAA59335	24%	31	Antioxidant enzyme
5	GST μ2	8.1	25	P10649	92%	75	Catalyzes the conjugation of glutathione to numerous potentially genotoxic compounds
6	GST μ2	7.3	25	P15626	91%	81	
7	Carbonyl reductase	9.1	26	NP_031647	95%	94	Catalyzes the NADPH-dependent reduction of ketones on steroids and prostaglandins
8	GTP-binding protein β-chain	7.6	35	NP_034440	50%	41	Involved in signal transduction
9	Annexin II	7.6	38	AAN86740	80%	90	Ca^{2+}-dependent phopholipid-binding protein, mediates corticosteroid activity and plays role in secretion
9	Lactate dehydrogenase	7.6	36	CAA26360	24%	19	Metabolic enzyme, converts lactate to pyruvate
10	Glyceraldehyde 3-phosphate dehydrogenase	8.4	36	AAH83149	69%	67	Enzyme in the glycolysis and gluconeogenesis pathways
	Malate dehydrogenase	8.9	36	CAA30274	48%	20	Metabolic enzyme of TCA cycle, converts malate to oxaloacetate
11	Aldolase A	8.3	39	AAA37210	65%	70	Metabolic enzyme of glycolysis pathway
12	Guanine nucleotide-binding protein	7.6	35	NP_034444	29%	39	Mediates the activation of cytosolic messengers in signal transduction pathway
13	Transketolase	7.2	68	AAH55336	44%	73	Reversible link between glycolysis and the pentose phosphate pathway
14	Methylmalonate semialdehyde dehydrogenase	8.5	57	AAG44988	42%	29	Responsible for the oxidative decarboxylation of malonate and methyl-malonate semialdehydes to acetyl- and propionyl-CoA
15	Pyruvate kinase	7.1	58	NP_598428	69%	82	Metabolic enzyme, converts phosphoenol-pyruvate to pyruvate
16	Catalase	7.7	59	AAA66054	58%	54	Catalyzes the conversion of H_2O_2 into water and oxygen
17	Aldehyde dehydrogenase	7.9	54	NP_036051	52%	67	Acts in detoxifying wide variety of organic compounds, toxins, and pollutants
18	Thioether S-methyl transferase	6	30	S52102	52%	46	Metabolic enzyme
19	Antioxidant protein 2	5.7	24	AC53277	0.83	48	A member of a family of thiol-specific antioxidants
20	Carbonic anhydrase II	6.5	29	AAA37356	0.23	26	Facilitates the transport of carbon dioxide
21	Selenium-binding protein	5.8	53	Q91X87	56%	52	Participates in intra Golgi protein transport
22	Mouse secretory protein YM-1	5.6	44	AAB62394	45%	43	Secretory protein
23	Serum albumin	5.7	70	NP_033784	35%	36	Transporter of small molecules in the blood
24	Annexin I	7	39	NP_034860	77%	76	Carries anti-inflammatory role and regulates Ca^{2+}-phospholipid activity
25	Dihydropyrimidinase-related protein	6	62	1351260	43%	36	Involved in axonal growth
26	ER60 protease	5.8	57	JC2385	49%	70	Cysteine protease of the endoplasmic reticulum
27	Protein disulfide isomerase	6	56	AAA39906	0.32	57	Resident foldase of the endoplasmic recticulum, catalyzes the formation and isomerization of disulphide bonds during protein folding

[a] Nitrated proteins found on two-dimensional gel of OVA-sensitized and challenged mice lung (shown in Fig 4) were identified by peptide mass mapping using product-ion (tandem mass) spectra. These proteins are shown with pI, molecular mass, accession no., percentage coverage, number of peptides matched, and a brief description of the function of the protein.
[b] Corresponds to numbered spots in Fig. 4, *B* and *D*.

A

B
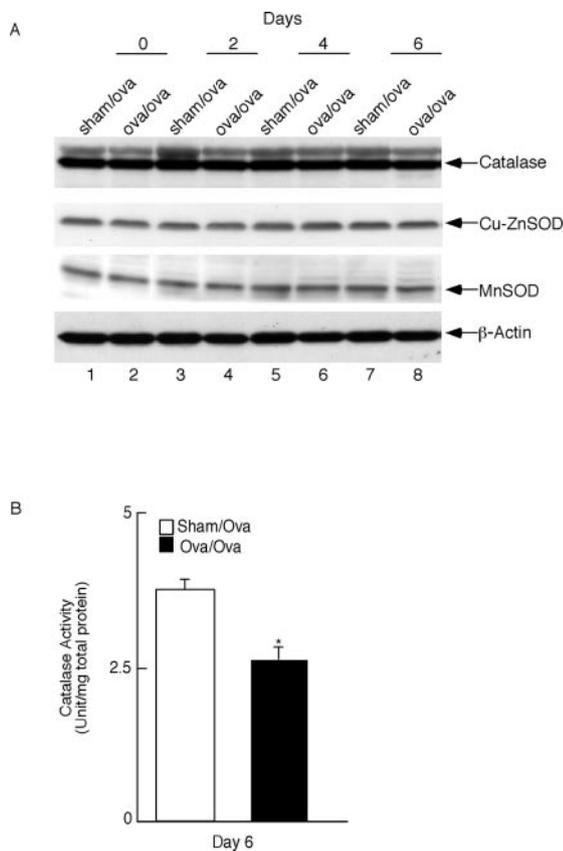
FIGURE 5. *A*, Antioxidant protein level in OVA/OVA mouse lung and corresponding control. Whole lung lysate from OVA/OVA mice at days 0, 2, 4, and 6 (*lanes 2, 4, 6,* and *8*) and corresponding controls at respective days (*lanes 1, 3, 5,* and *7*) were analyzed by Western blot using anti-catalase, anti-Cu/Zn-SOD, and anti-MnSOD Ab. There is no significant change in the levels of protein expression. *B*, Decrease of catalase activity in OVA/OVA mouse lung at day 6 of allergen challenge compared with control. Catalase activity (expressed in units per milligram of total protein) is significantly decreased in asthmatic mouse lung at day 6 after allergen challenge, compared with control. ∗, Indicates $p < 0.05$. Values are mean ± SEM of three experiments.

epithelial cells freshly obtained by bronchial brushings of control and asthmatic individuals did not show any significant change in protein levels (Fig. 6*B*). To investigate the nitration of catalase in human asthma, protein was immunoprecipitated with anti-catalase Ab from lysates of bronchial epithelial cells freshly obtained from asthmatic and healthy airways. The immunocomplex was resolved on a 10% gel, and the immunoblot was probed with an anti-nitrotyrosine Ab. Immunoprecipitated catalase from asthmatic airway epithelium was detected by anti-nitrotyrosine Ab, but not in healthy control. The integrity of the protein was confirmed by Western blot analysis with anti-catalase Ab (Fig. 6, *C* and *D*). Isolated catalase, either untreated or nitrated with tetranitromethane, were used as negative and positive controls, respectively.

Oxidation of catalase in human asthmatic airway epithelial cells

To quantitate oxidative modifications of catalase in asthmatic airway epithelial cells, cells were recovered during bronchoscopy, lysed, and catalase purified by immunoprecipitation. Molecular markers of multiple distinct oxidative pathways, including nitrotyrosine and Cl-Y, were quantified by stable isotope dilution tandem MS (Table II). Two oxidant modifications were dominant: 1) chlorination of tyrosine, a specific molecular marker for peroxidase-catalyzed halogenation; and 2) oxidative cross-linking of ty-

rosine as monitored by dityrosine, a product of tyrosyl radical. In contrast, oxidation of phenylalanine to the nonphysiologic tyrosine isomers, metatyrosine, and orthotyrosine, was scant, suggesting that exposure to hydroxyl radical-like oxidants through Fenton/Haber-Weiss reaction mechanisms (i.e., redox-active transition metal ion-catalyzed oxidation) was not significant. Consistent with our immunodetection studies, nitration of tyrosine was present in catalase recovered from asthmatic airway epithelial cells, indicating exposure to nitrating oxidants such as peroxynitrite/peroxycarboxynitrite or peroxidase-mediated reactive nitrogen species. It is important to note that asthmatics in this study were clinically mild. In this context, loss of catalase activity may be greater in asthma exacerbation and in severe asthma conditions in which generation of ROS and RNS is greatly increased.

In vitro modification of catalase and loss of activity

To gain insight into the potential mechanism of the loss of catalase activity in asthma, catalase was treated with HOCl (0–100 μM) in vitro, a range that represents physiologic levels to pathologic levels, as seen in inflammation (29). Activity assay of the catalase following exposure to HOCl was performed, as well as Cl-Y quantitation. Catalase activity was decreased in a dose-dependent manner with HOCl treatment, concomitant with a dose-dependent increase of Cl-Y formation (Fig. 7*A*). The first detectable loss of activity occurred at a 4:1 molar ratio of HOCl to catalase, a point at which 0.050 ± 0.005 mmol/mol Cl-Y/Y was measured. Higher concentrations of HOCl lead to lower enzyme activity and higher amounts of Cl-Y/Y. The enzyme activity was nearly completely lost with the 30 μM HOCl treatment (39:1 molar ratio of HOCl to catalase protein). At this treatment point, the production of Cl-Y/Y was 0.57 ± 0.09 mmol/mol, a level well within the range detected in catalase protein from human asthmatic airway epithelial cells (Table II). This finding suggests that the level of reactive chlorinating species present in human asthmatic airways is within the range used in this in vitro study, i.e., 3–100 mM.

To determine whether catalase is a target of peroxidase-mediated modification, catalase was exposed to reactive chlorinating (or nitrating) species by MPO-H_2O_2-Cl^- (or nitrogen dioxide radical$^-$) system. Because catalase and MPO compete for the same substrate (H_2O_2) and the former has a higher affinity for substrate, catalase was first inactivated by aminotriazole. Subsequent to inactivation and exposure to the MPO system, catalase was evaluated for total Cl-Y and nitrotyrosine. Both chlorination (0.051 ± 0.001 mmol/mol; $p < 0.001$) and nitration (0.77 ± 0.02 mmol/mol; $p < 0.00$) were observed with the MPO-mediated oxidation system. Although activity analysis could not be performed in this experiment because the catalase was inactivated before oxidation, these results show that catalase is a target for peroxidase-mediated modification. Overall, the levels of chlorination found in catalase of human airway epithelial cells in vivo (Table II), together with our in vitro studies indicate that high levels (micromolar range) of reactive chlorinating species are present in the asthmatic airway epithelial cells.

Finally, a series of MS experiments were conducted to identify the site(s) of oxidative modification in catalase using in vitro reactions. HOCl-inactivated catalase and native catalase from the dose-dependent experiments were separated on SDS-PAGE and sequenced by both LC-tandem MS and MALDI-TOF. These sequencing experiments covered ~70% of the protein sequence, including 12 of the 20 tyrosine residues and three of the four cysteine residues. Tyrosine modifications were not detected. The modification of C377, however, was discovered and characterized as shown in Fig. 7, *C* and *D*. This modification produces a cysteic acid with a corresponding increase of 48 kDa in the tryptic peptide Leu[366] to

FIGURE 6. *A*, Decrease of catalase activity in human asthmatic BALF. Catalase activity (expressed in mU/ml ELF) is present in asthmatic BALF but is less than controls ($p < 0.05$). *B*, Level of catalase in human airway epithelial cells. Catalase protein expression was directly evaluated in airway epithelial cells freshly obtained at bronchoscopy from healthy controls (*lanes 1* and *2*) or asthmatic airways (*lanes 3* and *4*) by Western blot analysis. The graph shows no significant change in the levels of protein expression in asthmatic samples ($n = 5$) compared with control ($n = 3$); $p = 0.18$. *C*, Verification of catalase nitration in asthmatic airway epithelial cells compared with control. Airway epithelial cell lysates from control (*lane 1*) and asthmatic individual (*lane 2*) were immunoprecipitated with anti-catalase Ab and analyzed by Western blot for anti-nitrotyrosine immunoreactivity. Pure nitrated catalase (*lane 3*) is the positive control, and untreated pure catalase serves as negative control (*lane 4*). Western analysis with anti-catalase Ab (*lower panel*) represents protein integrity. All data are representative of at least three experiments from different individuals. *D*, Densitometric analysis shows that nitrated catalase relative to total catalase is significantly increased in asthmatic individuals compared with control. ∗, Indicates $p < 0.05$.
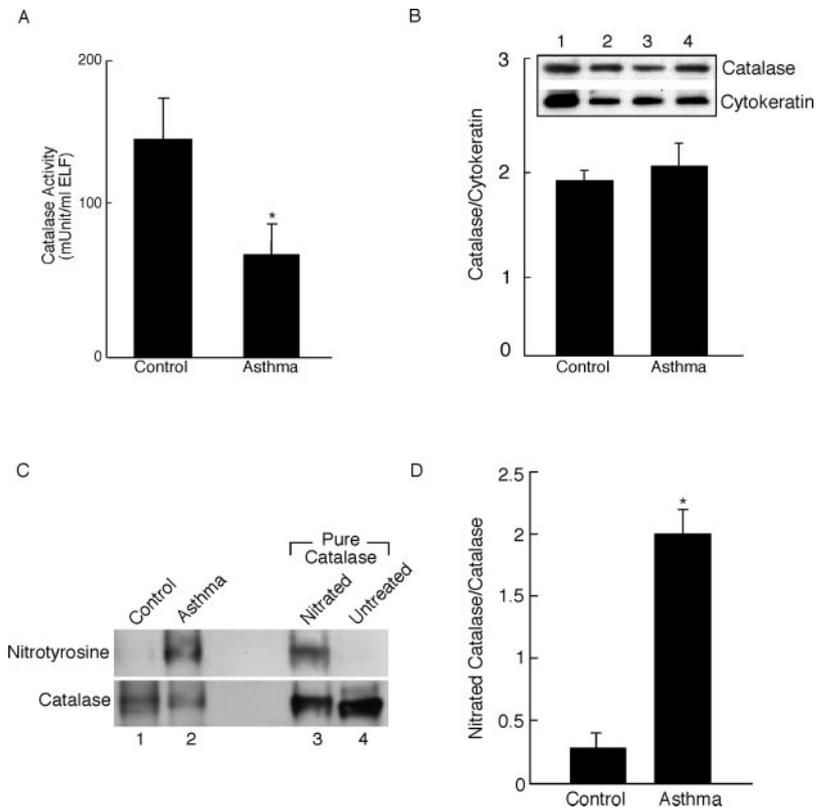
Arg[380]. The CID spectra (Fig. 7*C*) clearly place the site of modification. No other modified cysteine residues were observed. In fact, it was striking to note that the MALDI-TOF spectra of all four catalase digests, ranging from untreated-full active to the highly oxidized-completely inactive were nearly superimposable except for the changes in this peptide (data not shown). Importantly, the C377 oxidation product was seen in high abundance, and the relative amounts of the oxidized vs unoxidized peptides showed a dose-dependent increase in the oxidized form with a corresponding decrease in the unoxidized form that correlated with the loss of activity seen in Fig. 7*A*.

Discussion

This study identifies the nitrotyrosine proteome in the experimental allergen-induced murine model of asthma, and the specific proteins that are susceptible to oxidative modifications in vivo. As previously shown in murine and human allergen challenge studies, tyrosine nitration increases following allergen exposure of sensitized mice or atopic asthmatic humans (1, 17, 22, 52). The temporal sequence of events and airway localization of nitrotyrosine, in this and previous studies (17), clearly support a link between eosinophilic infiltration and oxidation events and suggest that eosinophils may contribute to the NO-derived oxidants in asthma (18).

Tyrosine nitration is a well-established protein modification that occurs in diseases associated with oxidative and nitrative stress,

including asthma (5, 25, 26, 53, 54). Although levels of nitrotyrosine increase over time of an asthmatic response to allergen, the total NO_X levels, which are considered measures of NO formation, were not greater than in control mouse lungs. Previous evaluation of human asthma over the time of allergen challenge showed that nitrotyrosine, exhaled NO, and nitrate in lung lavage fluid, but not nitrite, increased 48 h after a localized allergen challenge in the asthmatic airway. Thus, NO synthesis by iNOS and consumption by oxidant reactions/peroxidases appear to increase concomitantly over the time of an allergen-induced asthmatic response in humans (17). In this study, although iNOS was induced at days 4 and 6 following allergen challenge, arginase I expression was also induced, consistent with a previous study (47). Arginase and NOS proteins share the common substrate arginine. Although arginase has a lower affinity for substrate compared with NOS proteins, it has a higher catabolic reaction rate constant. Taking into account catalytic reaction rate and substrate affinity, arginase likely plays a regulatory role in NO synthesis by modulating the availability of arginine for the NOS proteins (48, 55–60). Thus, lack of increase of NO_X in this experimental model of asthma may be related in part to decreased enzymatic NO synthesis mediated by the concomitant induction of arginase I and iNOS. Alternatively, the greater consumption of nitrite for tyrosine nitration may also account for the lack of increase of other NO-reaction products.

The proteomic approach to identify proteins modified by exposure to RNS in the murine model of experimental asthma permits

Table II. *Quantification of oxidative modification of catalase in human asthmatic airway epithelial cells[a]*

NO_2Y/Y	BrY/Y	ClY/Y	mY/F	oY/F	DiY/Y
0.32 ± 0.06	0.06 ± 0.005	5.4 ± 2.5	0.04 ± 0.04	0.07 ± 0.01	1.41 ± 0.3

[a] Data represent the range of values observed in catalase isolated from epithelial cells from mild asthmatic subjects ($n = 4$). Results are normalized to the content of the appropriate precursor amino acid (mmol oxidation product/mol precursor (Y) and (F)), which were determined in the same analysis. Y, Tyrosine; NO_2Y, nitrotyrosine; BrY, bromotyrosine; DiY, dityrosine; oY, o-tyrosine; mY, m-tyrosine; F, phenylalanine.
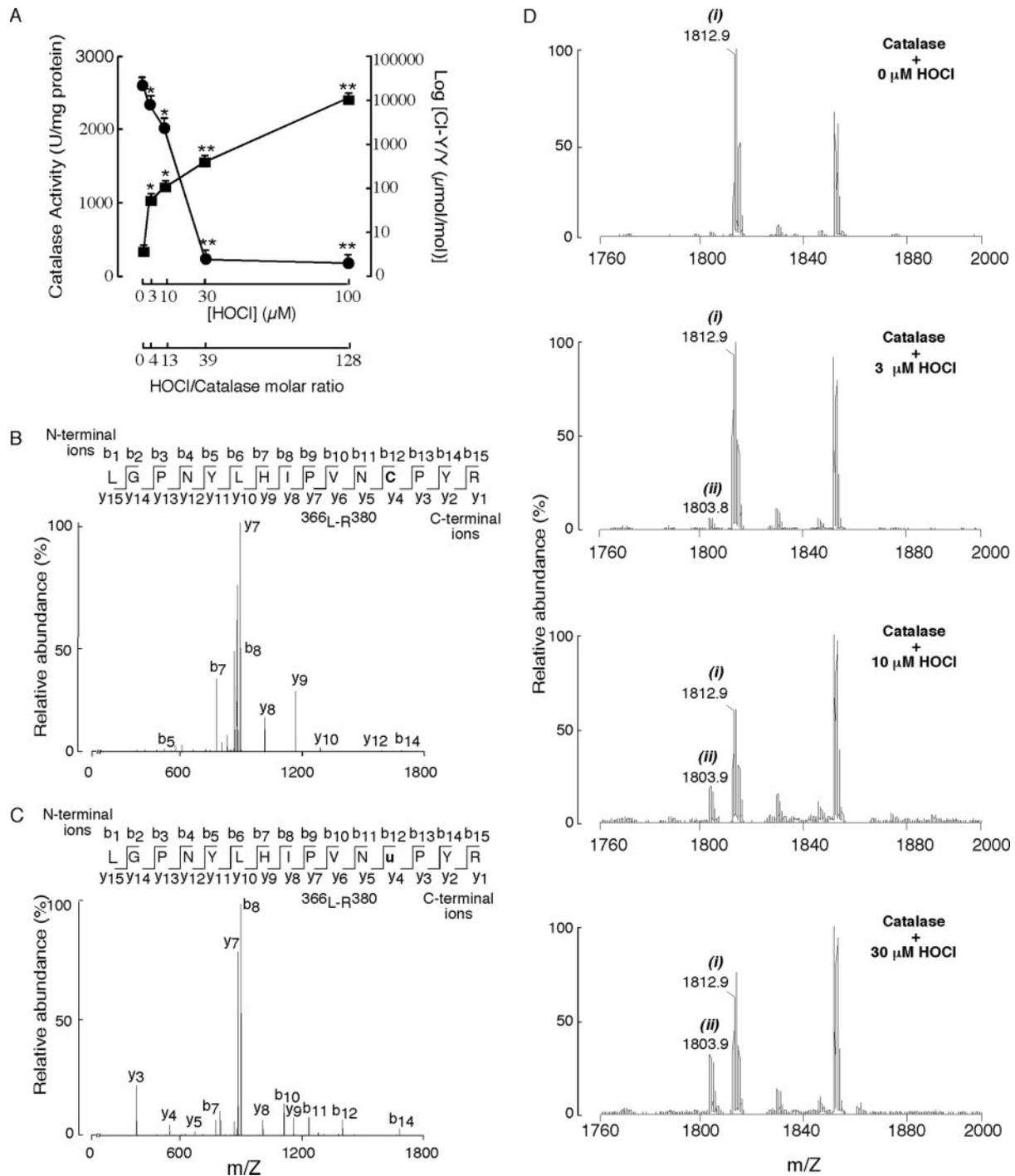
FIGURE 7. *A*, Loss of catalase activity and increase in Cl-Y formation with increasing dose of HOCl. Catalase (100 μg for each reaction) was exposed to reactive chlorinating species with increasing amounts of HOCl (0–100 μM). The modified catalase from each reaction was subjected to activity analysis and quantitation for Cl-Y formation. Catalase activity (●) was significantly decreased (linear scale) with increasing concentration of HOCl (linear scale), showing sharp decrease between 10 and 30 μM HOCl concentration. Cl-Y formation (■) increased (plotted in logarithmic scale) with increasing concentration of HOCl, reaching peak at 100 μM HOCl. Secondary *x*-axis represents molar ratio of HOCl:Catalase (linear scale). *, Indicates $p < 0.05$ and **, indicates $p < 0.01$. *B* and *C*, CID spectra of peptides from unoxidized and oxidized catalase. The CID spectra were acquired in the LC-tandem MS analysis of in-gel tryptic digests of catalase bands for control and HOCl-oxidized samples. The spectra correspond to the doubly charged ion of the peptide Leu[366] to Arg[380] (L_{366}-R_{380}). Spectrum B is for the unoxidized peptide in which the cysteine residue is alkylated with iodoacetamide to add 57 kDa to give a peptide with a molecular mass of 1812.9 ($M+H^+$). Spectrum B is for the oxidized peptide in which the cysteine residue is converted to a cysteic acid. This modification adds 48 kDa to give a peptide with a molecular mass of 1803.9 ($M+H^+$). The CID spectrum is very informative and clearly places the mass difference at the C377 position through the y3 and y4 ions that are seen and the corresponding residue mass of 151 kDa for the cysteic acid. *D*, MALDI-TOF spectra show the dose-dependent increase in the abundance of the oxidized C377 peptide relative to the unoxidized peptide. The C377-containing peptide was clearly seen in the MALDI-TOF analysis of the in-gel tryptic digests. The oxidized form (*ii*, m/z 1803.9) is readily detected in the 3-μM treatment and increases significantly in the 10- and 30-μM treatment. A corresponding decrease in the unoxidized form (*ii*, m/z 1812.9) is also seen. Based on these relative abundances, the relative amounts of the oxidized form progresses from 6% at 3-μM treatment, to 24% at-10 μM treatment, to 33% at 30-μM HOCl treatment. As noted above, the carbamidomethylation of the unoxidized cysteine in the sample processing means that the unoxidized form of the peptide is seen at a higher m/z than the oxidized form.

a sensitive means to study the potential involvement of RNS and ROS in vivo. On average, proteins are composed of 4% tyrosine residues, but evidence suggests that only a subset of the proteins are recognized by nitrotyrosine mAb in these biological systems. Interestingly, many of the proteins identified in this study were similar to those identified during the murine inflammatory response to LPS in vivo (40). This overlap is consistent with the concept that an innate property of the target protein or its location in the cell predisposes it toward nitration (61), and with recent studies by Suri et al. (62) that the sequence context in which nitrotyrosines exist participate in the presentation of the modified amino acid by the MHC class II-presenting cells. Similar to previous reports, many of the modified proteins are key enzymes for energy production, like pyruvate kinase, lactate dehydrogenase, malate dehydrogenase, aldolase A, and glyceraldehyde phosphate dehydrogenase, suggesting reduction of glycolysis and/or conversion to other metabolic pathways for energy within cells during the inflammatory response. Dihydropyrimidinase-related protein, which is involved in axonal growth and a target of protein nitration in Alzheimer's disease (63), is also identified as a target for nitration during asthma. Annexin II and III belong to the annexin superfamily of calcium and phospholipid-binding proteins (64), and annexin I is an important mediator of glucocorticoid action (65); all are found to be nitrated in the experimental model of asthma. Although the effect of nitration on annexin I is not known, further studies are warranted to determine whether glucocorticoid response during inflammation may be altered.

Notably, catalase, MnSOD, GST, antioxidant protein 2, and carbonic anhydrase II are nitrated in the murine model of asthma, although these enzymes are present in different compartments of the cell. Although a previous study showed that RBC of asthmatic children have lower catalase activity (66), the mechanism of the reduced activity was unknown. Nitration of MnSOD, which causes its inactivation in vitro (67), occurs in diseases like chronic rejection of the human renal allograft (68). MnSOD is nitrated in the asthmatic airway epithelial cells, but the dominant oxidant modifications are related to hydroxyl radical like oxidants presumably via Fenton or Haber-Weiss chemical events (37). Other studies have shown that catalase and GST activity are reduced by exposure to reactive nitrogen species in vitro (69, 70). Loss of catalase activity in a murine model of autoimmune disease that includes arthritis and vasculitis has also been linked to increased nitration, although the modification was not identified (69).

The identification of catalase as a selective target in our proteomic experiments led to additional in vivo and in vitro studies. Significant decrease in lung catalase activity was observed in vivo in the experimental murine model of asthma as well as in human asthmatic airway lining fluid. In human and murine lungs, loss of catalase activity was associated with corresponding increases in catalase nitrotyrosine content by immunodetection methods. The quantitation of a series of stable end products of protein oxidation, however, revealed a broader picture of the oxidative modification of catalase in vivo (Table II). Indeed, the most extensive modification measured was tyrosine chlorination, which was nearly 20-

fold more extensive than tyrosine nitration. In vitro exposure of catalase to reactive chlorinating oxidants led to significant Cl-Y formation and a profound dose-dependent inactivation of the enzyme. Importantly, these in vitro studies confirm that inactivation of catalase activity occurs at exposure levels to chlorinating oxidants well within the range that is observed in the human asthmatic airway. Both murine and human catalase contain a putative chlorination site (KXHY) at Tyr^{236} (71) (Fig. 8). This motif would be predicted to be particularly susceptible to HOCl-mediated chlorination based on formation of an N-ϵ chloramine intermediate on the lysine residue (71). LC-tandem MS and MALDI-TOF mapping experiments, thus far however, have failed to find specific tyrosine chlorination sites. In this context, it is notable that even the highest Cl-Y content of catalase that was measured in the various in vitro and in vivo experiments ranged up to ~5 mmol of Cl-Y/mol Y, which represents <0.5% modification of the total tyrosines within the enzyme. If all modification occurred at a single site, this Cl-Y content would be equivalent to 10% modification of that site, which would be detectable by our methods. We speculate that our inability to detect modified tyrosines in catalase may be due to low levels of Cl-Y and/or the distribution of those modifications among different tyrosine sites (Fig. 8).

Our MS analyses did find a cysteine residue (C377), oxidized in a specific dose-dependent manner with a corresponding loss of the unoxidized peptide. This cysteine is close to the active site of the enzyme-active site, although no specific link between this cysteine and catalase function has been previously made. In this study, this modification occurred in a dose-dependent fashion and to an extent that parallels the degree of enzyme inactivation. For example, our data show that when treated in vitro with molar ratio of 13-reactive chlorinating species to one catalytically active catalase tetramer, catalase lost ~20% of its activity. The Cl-Y content at this treatment was ~0.1 mmol of Cl-Y/mol tyrosine (0.01% of total tyrosine), but the ratio of the oxidized C377 peptide to the unoxidized form in the MALDI-TOF analyses is ~1:3, or 25%, modified.

Taken together with our and other previous studies (5, 16, 17, 25, 26, 37, 40, 53, 54, 68, 69, 72), these current findings are consistent with the general utility of Cl-Y and nitrotyrosine measurements in studies of protein oxidation. Specifically, these stable end products of protein oxidation are excellent measures of the degree of oxidation, accurately detect increasing oxidation in disease, and can be measured by isotope dilution LC-tandem MS methods. However, in the case of catalase, tyrosine modification itself is not likely a direct contributor to the loss of catalase activity, but rather is associated with another oxidative modification, i.e., C377 to cysteic acid. Notably, multiple residues are susceptible to oxidative modification by reactive chlorinating species, including thiols (e.g., Cys), amines (e.g., Lys), guanidinium-containing residues (Arg), imidazole (His), indole (Trp), and amides (Gln and Asn) (73). Thus, although the nitrotyrosine proteome evaluation identifies specific proteins oxidized in human inflammatory disease, identification does not necessarily imply loss of activity related to tyrosine modification. Similarly, given the fact that oxidative and

FIGURE 8. Sequence location (circles) of 20 tyrosines in catalase and active sites of enzymes shown. *, mark difference of tyrosine residues in murine and human catalase. Tyr^{358} (open circle in square) is proximal heme ligand and critical for enzyme activity. Cys^{377} (▲) is modified to cysteic acid, when reacted with reactive chlorinating oxidants. Catalase contains a putative chlorination site (KXHY) at Tyr^{236} (●).
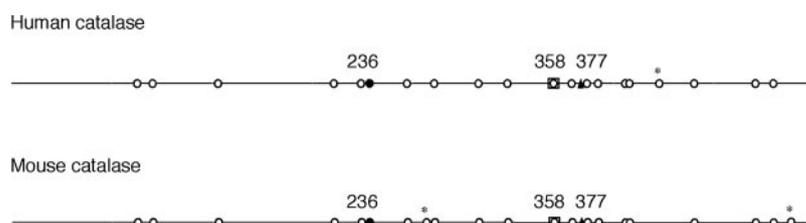
nitrative stress are linked to apoptosis and shedding of the airway epithelium in asthmatic airways (37), further studies are needed to determine whether oxidative modifications occur before, or consequent to, cell death.

In summary, these and previous findings (17, 37, 52, 74) suggest that the following sequence of oxidative events likely occurs in the asthmatic airway. During leukocyte activation, such as following allergen challenge, a respiratory burst occurs, generating O_2^- and its dismutation product H_2O_2. The H_2O_2 is used by peroxidase-mediated reaction that modifies susceptible proteins in the airway environment. Among those proteins is catalase, the antioxidant enzyme that would otherwise act to control the amounts of H_2O_2 present in the airway, allowing more H_2O_2 to accumulate at the site of inflammation. This loss of control further promotes peroxidase systems to produce nitrating, halogenating, and oxidizing species that amplify the inflammatory milieu of the asthmatic airway.

Acknowledgments

Disclosures

References

1. Iijima, H., A. Duguet, S. Y. Eum, Q. Hamid, and D. H. Eidelman. 2001. Nitric oxide and protein nitration are eosinophil dependent in allergen-challenged mice. *Am. J. Respir. Crit. Care Med.* 163: 1233–1240.
2. Calhoun, W. J., H. E. Reed, D. R. Moest, and C. A. Stevens. 1992. Enhanced superoxide production by alveolar macrophages and air-space cells, airway inflammation, and alveolar macrophage density changes after segmental antigen bronchoprovocation in allergic subjects. *Am. Rev. Respir. Dis.* 145: 317–325.
3. Gleich, G. J., E. A. Ottesen, K. M. Leiferman, and S. J. Ackerman. 1989. Eosinophils and human disease. *Int. Arch. Allergy Appl. Immunol.* 88: 59–62.
4. Horwitz, R. J., and W. W. Busse. 1995. Inflammation and asthma. *Clin. Chest Med.* 16: 583–602.
5. MacPherson, J. C., S. A. Comhair, S. C. Erzurum, D. F. Klein, M. F. Lipscomb, M. S. Kavuru, M. K. Samoszuk, and S. L. Hazen. 2001. Eosinophils are a major source of nitric oxide-derived oxidants in severe asthma: characterization of pathways available to eosinophils for generating reactive nitrogen species. *J. Immunol.* 166: 5763–5772.
6. Saleh, D., P. Ernst, S. Lim, P. J. Barnes, and A. Giaid. 1998. Increased formation of the potent oxidant peroxynitrite in the airways of asthmatic patients is associated with induction of nitric oxide synthase: effect of inhaled glucocorticoid. *FASEB J.* 12: 929–937.
7. Dweik, R. A., D. Laskowski, M. Ozkan, C. Farver, and S. C. Erzurum. 2001. High levels of exhaled nitric oxide (NO) and NO synthase III expression in lesional smooth muscle in lymphangioleiomyomatosis. *Am. J. Respir. Cell Mol. Biol.* 24: 414–418.
8. Guo, F. H., S. A. Comhair, S. Zheng, R. A. Dweik, N. T. Eissa, M. J. Thomassen, W. Calhoun, and S. C. Erzurum. 2000. Molecular mechanisms of increased nitric oxide (NO) in asthma: evidence for transcriptional and post-translational regulation of NO synthesis. *J. Immunol.* 164: 5970–5980.
9. Kharitonov, S. A., and P. J. Barnes. 2003. Nitric oxide, nitrotyrosine, and nitric oxide modulators in asthma and chronic obstructive pulmonary disease. *Curr. Allergy Asthma Rep.* 3: 121–129.
10. Khatri, S. B., M. Ozkan, K. McCarthy, D. Laskowski, J. Hammel, R. A. Dweik, and S. C. Erzurum. 2001. Alterations in exhaled gas profile during allergen-induced asthmatic response. *Am. J. Respir. Crit. Care Med.* 164: 1844–1848.
11. De Sanctis, G. T., J. A. MacLean, K. Hamada, S. Mehta, J. A. Scott, A. Jiao, C. N. Yandava, L. Kobzik, W. W. Wolyniec, A. J. Fabian, et al. 1999. Contribution of nitric oxide synthases 1, 2, and 3 to airway hyperresponsiveness and inflammation in a murine model of asthma. *J. Exp. Med.* 189: 1621–1630.
12. Kobzik, L., D. S. Bredt, C. J. Lowenstein, J. Drazen, B. Gaston, D. Sugarbaker, and J. S. Stamler. 1993. Nitric oxide synthase in human and rat lung: immunocytochemical and histochemical localization. *Am. J. Respir. Cell Mol. Biol.* 9: 371–377.
13. Calhoun, W. J., M. E. Bates, L. Schrader, J. B. Sedgwick, and W. W. Busse. 1992. Characteristics of peripheral blood eosinophils in patients with nocturnal asthma. *Am. Rev. Respir. Dis.* 145: 577–581.
14. Wu, W., M. K. Samoszuk, S. A. Comhair, M. J. Thomassen, C. F. Farver, R. A. Dweik, M. S. Kavuru, S. C. Erzurum, and S. L. Hazen. 2000. Eosinophils generate brominating oxidants in allergen-induced asthma. *J. Clin. Invest.* 105: 1455–1463.
15. Gaut, J. P., G. C. Yeh, H. D. Tran, J. Byun, J. P. Henderson, G. M. Richter, M. L. Brennan, A. J. Lusis, A. Belaaouaj, R. S. Hotchkiss, and J. W. Heinecke. 2001. Neutrophils employ the myeloperoxidase system to generate antimicrobial brominating and chlorinating oxidants during sepsis. *Proc. Natl. Acad. Sci. USA* 98: 11961–11966.
16. Hazen, S. L., and J. W. Heinecke. 1997. 3-Chlorotyrosine, a specific marker of myeloperoxidase-catalyzed oxidation, is markedly elevated in low density lipoprotein isolated from human atherosclerotic intima. *J. Clin. Invest.* 99: 2075–2081.
17. Dweik, R. A., S. A. Comhair, B. Gaston, F. B. Thunnissen, C. Farver, M. J. Thomassen, M. Kavuru, J. Hammel, H. M. Abu-Soud, and S. C. Erzurum. 2001. NO chemical events in the human airway during the immediate and late antigen-induced asthmatic response. *Proc. Natl. Acad. Sci. USA* 98: 2622–2627.
18. Brennan, M. L., W. Wu, X. Fu, Z. Shen, W. Song, H. Frost, C. Vadseth, L. Narine, E. Lenkiewicz, M. T. Borchers, et al. 2002. A tale of two controversies: defining both the role of peroxidases in nitrotyrosine formation in vivo using eosinophil peroxidase and myeloperoxidase-deficient mice, and the nature of peroxidase-generated reactive nitrogen species. *J. Biol. Chem.* 277: 17415–17427.
19. Eiserich, J. P., M. Hristova, C. E. Cross, A. D. Jones, B. A. Freeman, B. Halliwell, and A. van der Vliet. 1998. Formation of nitric oxide-derived inflammatory oxidants by myeloperoxidase in neutrophils. *Nature* 391: 393–397.
20. Wu, W., Y. Chen, and S. L. Hazen. 1999. Eosinophil peroxidase nitrates protein tyrosyl residues. Implications for oxidative damage by nitrating intermediates in eosinophilic inflammatory disorders. *J. Biol. Chem.* 274: 25933–25944.
21. van der Vliet, A., J. P. Eiserich, B. Halliwell, and C. E. Cross. 1997. Formation of reactive nitrogen species during peroxidase-catalyzed oxidation of nitrite: a potential additional mechanism of nitric oxide-dependent toxicity. *J. Biol. Chem.* 272: 7617–7625.
22. Andreadis, A. A., S. L. Hazen, S. A. Comhair, and S. C. Erzurum. 2003. Oxidative and nitrosative events in asthma. *Free Radical Biol. Med.* 35: 213–225.
23. Duguet, A., H. Iijima, S. Y. Eum, Q. Hamid, and D. H. Eidelman. 2001. Eosinophil peroxidase mediates protein nitration in allergic airway inflammation in mice. *Am. J. Respir. Crit. Care Med.* 164: 1119–1126.
24. Beckman, J. S., and W. H. Koppenol. 1996. Nitric oxide, superoxide, and peroxynitrite: the good, the bad, and ugly. *Am. J. Physiol.* 271: C1424–C1437.
25. Castegna, A., V. Thongboonkerd, J. B. Klein, B. Lynn, W. R. Markesbery, and D. A. Butterfield. 2003. Proteomic identification of nitrated proteins in Alzheimer's disease brain. *J. Neurochem.* 85: 1394–1401.
26. Horiguchi, T., K. Uryu, B. I. Giasson, H. Ischiropoulos, R. LightFoot, C. Bellmann, C. Richter-Landsberg, V. M. Lee, and J. Q. Trojanowski. 2003. Nitration of tau protein is linked to neurodegeneration in tauopathies. *Am. J. Pathol.* 163: 1021–1031.
27. Turko, I. V., and F. Murad. 2002. Protein nitration in cardiovascular diseases. *Pharmacol. Rev.* 54: 619–634.
28. Zheng, L., B. Nukuna, M. L. Brennan, M. Sun, M. Goormastic, M. Settle, D. Schmitt, X. Fu, L. Thomson, P. L. Fox, et al. 2004. Apolipoprotein A-I is a selective target for myeloperoxidase-catalyzed oxidation and functional impairment in subjects with cardiovascular disease. *J. Clin. Invest.* 114: 529–541.
29. Zheng, L., M. Settle, G. Brubaker, D. Schmitt, S. L. Hazen, J. D. Smith, and M. Kinter. 2005. Localization of nitration and chlorination sites on apolipoprotein A-I catalyzed by myeloperoxidase in human atheroma and associated oxidative impairment in ABCA1-dependent cholesterol efflux from macrophages. *J. Biol. Chem.* 280: 38–47.
30. Aronica, M. A., A. L. Mora, D. B. Mitchell, P. W. Finn, J. E. Johnson, J. R. Sheller, and M. R. Boothby. 1999. Preferential role for NF-κB/Rel signaling in the type 1 but not type 2 T cell-dependent immune response in vivo. *J. Immunol.* 163: 5116–5124.
31. De Raeve, H. R., F. B. Thunnissen, F. T. Kaneko, F. H. Guo, M. Lewis, M. S. Kavuru, M. Secic, M. J. Thomassen, and S. C. Erzurum. 1997. Decreased Cu,Zn-SOD activity in asthmatic airway epithelium: correction by inhaled corticosteroid in vivo. *Am. J. Physiol.* 272: L148–L154.
32. Comhair, S. A., M. J. Lewis, P. R. Bhathena, J. P. Hammel, and S. C. Erzurum. 1999. Increased glutathione and glutathione peroxidase in lungs of individuals with chronic beryllium disease. *Am. J. Respir. Crit. Care Med.* 159: 1824–1829.
33. Rennard, S. I., G. Basset, D. Lecossier, K. M. O'Donnell, P. Pinkston, P. G. Martin, and R. G. Crystal. 1986. Estimation of volume of epithelial lining fluid recovered by lavage using urea as marker of dilution. *J. Appl. Physiol.* 60: 532–538.
34. Machado, R. F., M. V. Londhe Nerkar, R. A. Dweik, J. Hammel, A. Janocha, J. Pyle, D. Laskowski, C. Jennings, A. C. Arroliga, and S. C. Erzurum. 2004. Nitric oxide and pulmonary arterial pressures in pulmonary hypertension. *Free Radical Biol. Med.* 37: 1010–1017.
35. Guo, F. H., K. Uetani, S. J. Haque, B. R. Williams, R. A. Dweik, F. B. Thunnissen, W. Calhoun, and S. C. Erzurum. 1997. Interferon γ and interleukin 4 stimulate prolonged expression of inducible nitric oxide synthase in human airway epithelium through synthesis of soluble mediators. *J. Clin. Invest.* 100: 829–838.
36. Aebi, H. 1984. Catalase in vitro. *Methods Enzymol.* 105: 121–126.
37. Comhair, S. A., W. Xu, S. Ghosh, F. B. Thunnissen, A. Almasan, W. J. Calhoun, A. J. Janocha, L. Zheng, S. L. Hazen, and S. C. Erzurum. 2005. Superoxide dismutase inactivation in pathophysiology of asthmatic airway remodeling and reactivity. *Am. J. Pathol.* 166: 663–674.
38. Heinecke, J. W., W. Li, G. A. Francis, and J. A. Goldstein. 1993. Tyrosyl radical generated by myeloperoxidase catalyzes the oxidative cross-linking of proteins. *J. Clin. Invest.* 91: 2866–2872.
39. Laemmli, U. K. 1970. Cleavage of structural proteins during the assembly of the head of bacteriophage T4. *Nature* 227: 680–685.
40. Aulak, K. S., M. Miyagi, L. Yan, K. A. West, D. Massillon, J. W. Crabb, and D. J. Stuehr. 2001. Proteomic method identifies proteins nitrated in vivo during inflammatory challenge. *Proc. Natl. Acad. Sci. USA* 98: 12056–12061.

41. Conway, J. P., and M. Kinter. 2005. Proteomic and transcriptomic analyses of macrophages with an increased resistance to oxidized low density lipoprotein (oxLDL)-induced cytotoxicity generated by chronic exposure to oxLDL. *Mol. Cell. Proteomics* 4: 1522–1540.

42. Ducret, A., I. Van Oostveen, J. K. Eng, J. R. Yates, 3rd, and R. Aebersold. 1998. High throughput protein characterization by automated reverse-phase chromatography/electrospray tandem mass spectrometry. *Protein Sci.* 7: 706–719.

43. Aronica, M. A., S. McCarthy, S. Swaidani, D. Mitchell, M. Goral, J. R. Sheller, and M. Boothby. 2004. Recall helper T cell response: T helper 1 cell-resistant allergic susceptibility without biasing uncommitted CD4 T cells. *Am. J. Respir. Crit. Care Med.* 169: 587–595.

44. Foster, P. S., S. P. Hogan, A. J. Ramsay, K. I. Matthaei, and I. G. Young. 1996. Interleukin 5 deficiency abolishes eosinophilia, airways hyperreactivity, and lung damage in a mouse asthma model. *J. Exp. Med.* 183: 195–201.

45. De Monchy, J. G., H. F. Kauffman, P. Venge, G. H. Koeter, H. M. Jansen, H. J. Sluiter, and K. De Vries. 1985. Bronchoalveolar eosinophilia during allergen-induced late asthmatic reactions. *Am. Rev. Respir. Dis.* 131: 373–376.

46. Ohashi, Y., S. Motojima, T. Fukuda, and S. Makino. 1992. Airway hyperresponsiveness, increased intracellular spaces of bronchial epithelium, and increased infiltration of eosinophils and lymphocytes in bronchial mucosa in asthma. *Am. Rev. Respir. Dis.* 145: 1469–1476.

47. Zimmermann, N., N. E. King, J. Laporte, M. Yang, A. Mishra, S. M. Pope, E. E. Muntel, D. P. Witte, A. A. Pegg, P. S. Foster, et al. 2003. Dissection of experimental asthma with DNA microarray analysis identifies arginase in asthma pathogenesis. *J. Clin. Invest.* 111: 1863–1874.

48. Wu, G., and S. M. Morris, Jr. 1998. Arginine metabolism: nitric oxide and beyond. *Biochem J.* 336(Pt 1): 1–17.

49. Xu, W., F. T. Kaneko, S. Zheng, S. A. Comhair, A. J. Janocha, T. Goggans, F. B. Thunnissen, C. Farver, S. L. Hazen, C. Jennings, et al. 2004. Increased arginase II and decreased NO synthesis in endothelial cells of patients with pulmonary arterial hypertension. *FASEB J.* 18: 1746–1748.

50. Hamid, Q., D. R. Springall, V. Riveros-Moreno, P. Chanez, P. Howarth, A. Redington, J. Bousquet, P. Godard, S. Holgate, and J. M. Polak. 1993. Induction of nitric oxide synthase in asthma. *Lancet* 342: 1510–1513.

51. Comhair, S. A., P. R. Bhathena, C. Farver, F. B. Thunnissen, and S. C. Erzurum. 2001. Extracellular glutathione peroxidase induction in asthmatic lungs: evidence for redox regulation of expression in human airway epithelial cells. *FASEB J.* 15: 70–78.

52. Hazen, S. L., R. Zhang, Z. Shen, W. Wu, E. A. Podrez, J. C. MacPherson, D. Schmitt, S. N. Mitra, C. Mukhopadhyay, Y. Chen, et al. 1999. Formation of nitric oxide-derived oxidants by myeloperoxidase in monocytes: pathways for monocyte-mediated protein nitration and lipid peroxidation in vivo. *Circ Res.* 85: 950–958.

53. Keshavarzian, A., A. Banan, A. Farhadi, S. Komanduri, E. Mutlu, Y. Zhang, and J. Z. Fields. 2003. Increases in free radicals and cytoskeletal protein oxidation and nitration in the colon of patients with inflammatory bowel disease. *Gut* 52: 720–728.

54. Nikov, G., V. Bhat, J. S. Wishnok, and S. R. Tannenbaum. 2003. Analysis of nitrated proteins by nitrotyrosine-specific affinity probes and mass spectrometry. *Anal. Biochem.* 320: 214–222.

55. Vodovotz, Y., N. S. Kwon, M. Pospischil, J. Manning, J. Paik, and C. Nathan. 1994. Inactivation of nitric oxide synthase after prolonged incubation of mouse macrophages with IFN-γ and bacterial lipopolysaccharide. *J. Immunol.* 152: 4110–4118.

56. Morris, S. M., Jr. 2002. Regulation of enzymes of the urea cycle and arginine metabolism. *Annu. Rev. Nutr.* 22: 87–105.

57. Kung, J. T., S. B. Brooks, J. P. Jakway, L. L. Leonard, and D. W. Talmage. 1977. Suppression of in vitro cytotoxic response by macrophages due to induced arginase. *J. Exp. Med.* 146: 665–672.

58. Hey, C., J. L. Boucher, S. Vadon-Le Goff, G. Ketterer, I. Wessler, and K. Racke. 1997. Inhibition of arginase in rat and rabbit alveolar macrophages by N omega-hydroxy-D,L-indospicine, effects on L-arginine utilization by nitric oxide synthase. *Br. J. Pharmacol.* 121: 395–400.

59. Gotoh, T., and M. Mori. 1999. Arginase II downregulates nitric oxide (NO) production and prevents NO-mediated apoptosis in murine macrophage-derived RAW 264.7 cells. *J. Cell Biol.* 144: 427–434.

60. Currie, G. A., L. Gyure, and L. Cifuentes. 1979. Microenvironmental arginine depletion by macrophages in vivo. *Br. J. Cancer.* 39: 613–620.

61. Souza, J. M., E. Daikhin, M. Yudkoff, C. S. Raman, and H. Ischiropoulos. 1999. Factors determining the selectivity of protein tyrosine nitration. *Arch. Biochem. Biophys.* 371: 169–178.

62. Suri, A., J. J. Walters, O. Kanagawa, M. L. Gross, and E. R. Unanue. 2003. Specificity of peptide selection by antigen-presenting cells homozygous or heterozygous for expression of class II MHC molecules: the lack of competition. *Proc. Natl. Acad. Sci. USA* 100: 5330–5335.

63. Castegna, A., M. Aksenov, V. Thongboonkerd, J. B. Klein, W. M. Pierce, R. Booze, W. R. Markesbery, and D. A. Butterfield. 2002. Proteomic identification of oxidatively modified proteins in Alzheimer's disease brain. Part II: Dihydropyrimidinase-related protein 2, α-enolase and heat shock cognate 71. *J Neurochem.* 82: 1524–1532.

64. Sopkova, J., C. Raguenes-Nicol, M. Vincent, A. Chevalier, A. Lewit-Bentley, F. Russo-Marie, and J. Gallay. 2002. Ca²⁺ and membrane binding to annexin 3 modulate the structure and dynamics of its N terminus and domain III. *Protein Sci.* 11: 1613–1625.

65. Cover, P. O., F. Baanah-Jones, C. D. John, and J. C. Buckingham. 2002. Annexin 1 (lipocortin 1) mimics inhibitory effects of glucocorticoids on testosterone secretion and enhances effects of interleukin-1β. *Endocrine* 18: 33–39.

66. Novak, Z., I. Nemeth, K. Gyurkovits, S. I. Varga, and B. Matkovics. 1991. Examination of the role of oxygen free radicals in bronchial asthma in childhood. *Clin. Chim. Acta* 201: 247–251.

67. Crow, J. P. 1999. Manganese and iron porphyrins catalyze peroxynitrite decomposition and simultaneously increase nitration and oxidant yield: implications for their use as peroxynitrite scavengers in vivo. *Arch. Biochem. Biophys.* 371: 41–52.

68. MacMillan-Crow, L. A., J. P. Crow, J. D. Kerby, J. S. Beckman, and J. A. Thompson. 1996. Nitration and inactivation of manganese superoxide dismutase in chronic rejection of human renal allografts. *Proc. Natl. Acad. Sci. USA* 93: 11853–11858.

69. Keng, T., C. T. Privalle, G. S. Gilkeson, and J. B. Weinberg. 2000. Peroxynitrite formation and decreased catalase activity in autoimmune MRL-*lpr/lpr* mice. *Mol. Med.* 6: 779–792.

70. Wong, P. S., J. P. Eiserich, S. Reddy, C. L. Lopez, C. E. Cross, and A. van der Vliet. 2001. Inactivation of glutathione *S*-transferases by nitric oxide-derived oxidants: exploring a role for tyrosine nitration. *Arch. Biochem. Biophys.* 394: 216–228.

71. Bergt, C., X. Fu, N. P. Huq, J. Kao, and J. W. Heinecke. 2004. Lysine residues direct the chlorination of tyrosines in YXXK motifs of apolipoprotein A-I when hypochlorous acid oxidizes high density lipoprotein. *J. Biol. Chem.* 279: 7856–7866.

72. Ischiropoulos, H. 1998. Biological tyrosine nitration: a pathophysiological function of nitric oxide and reactive oxygen species. *Arch. Biochem. Biophys.* 356: 1–11.

73. Podrez, E. A., H. M. Abu-Soud, and S. L. Hazen. 2000. Myeloperoxidase-generated oxidants and atherosclerosis. *Free Radical Biol Med.* 28: 1717–1725.

74. Comhair, S. A., P. R. Bhathena, R. A. Dweik, M. Kavuru, and S. C. Erzurum. 2000. Rapid loss of superoxide dismutase activity during antigen-induced asthmatic response. *Lancet* 355: 624.